



HAL
open science

Near-field optical spectroscopy using an incoherent light source

L. Aigouy, F X Andréani, A C Boccara, J C Rivoal, J A Porto, R. Carminati, J.-J Greffet, R. Megy

► **To cite this version:**

L. Aigouy, F X Andréani, A C Boccara, J C Rivoal, J A Porto, et al.. Near-field optical spectroscopy using an incoherent light source. *Applied Physics Letters*, 2000, 76 (4), pp.397. 10.1063/1.125766 . hal-01621663

HAL Id: hal-01621663

<https://hal.science/hal-01621663>

Submitted on 29 Aug 2022

HAL is a multi-disciplinary open access archive for the deposit and dissemination of scientific research documents, whether they are published or not. The documents may come from teaching and research institutions in France or abroad, or from public or private research centers.

L'archive ouverte pluridisciplinaire **HAL**, est destinée au dépôt et à la diffusion de documents scientifiques de niveau recherche, publiés ou non, émanant des établissements d'enseignement et de recherche français ou étrangers, des laboratoires publics ou privés.



Distributed under a Creative Commons Attribution - NonCommercial 4.0 International License

Near-field optical spectroscopy using an incoherent light source

L. Aigouy,^{a)} F. X. Andréani, A. C. Boccara, and J. C. Rivoal^{b)}

Spectroscopie en Lumière Polarisée (UPR 5 du CNRS), E.S.P.C.I., 10 rue Vauquelin, 75231 Paris Cedex 5, France

J. A. Porto, R. Carminati, and J.-J. Greffet

Laboratoire d'Energétique Moléculaire et Macroscopique, Combustion (UPR 288 du CNRS), Ecole Centrale de Paris, 92295 Châtenay-Malabry Cedex, France

R. Mégy

Institut d'Electronique Fondamentale (UMR 8622 du CNRS), Batiment 220, Université Paris-Sud, 91405 Orsay, France

(Received 2 August 1999; accepted for publication 23 November 1999)

We present a method to perform near-field optical spectroscopy. It consists of an apertureless near-field optical microscope combined with an incoherent light source and a monochromator. We show that the optical response of the tip depends both on the wavelength and the tip apex shape. The experimental optical response of the tips is in good agreement with the predicted theoretical one. The near-field optical spectrum obtained on a gold island in the visible spectrum range ($\lambda = 400\text{--}600\text{ nm}$) is presented and shows that the method is reliable to perform spectroscopic measurements on submicrometer-sized objects. © 2000 American Institute of Physics. [S0003-6951(00)02204-X]

Scanning near-field optical microscopy (SNOM) is a technique that allows to image the details of objects with a subwavelength resolution.¹ Since its implementation, there has been a continuous trend to extend the applicability of this technique to different wavelengths: from the microwave at the beginning,² to the visible,³ and the mid infrared.⁴ Spectroscopic applications of the technique have also been demonstrated. They mainly concern emission processes such as luminescence,⁵ Raman spectroscopy,⁶ and more recently two-photon fluorescence.⁷ Results on absorption processes are more scattered and only Klar *et al.*⁸ have been able to perform spectroscopic measurements of the optical response of gold nanoparticles using a tunable laser. However, the use of a tunable laser over a continuous wide range of wavelength is expensive and quite difficult to achieve in a routine way.

In this letter, we present a method that allows to perform near-field spectroscopy with a broadband source coupled with a grating spectrometer. We have used an apertureless SNOM^{4,9,10} with an electrochemically etched tungsten tip as a probe. We first study the optical response of the tip as a function of the wavelength. Using a simple theoretical model, we show that the electromagnetic coupling between the tip and the light depends both on the wavelength and the tip apex shape. We have experimentally observed this effect on two tips having a different cone angle, and the measured optical dependencies are in good agreement with theoretical predictions. Finally, we also show that the method allows to measure the optical response of submicrometer-sized objects, and more particularly to determine the position of absorption edges or transitions energies.

The general operating mode of the apertureless SNOM has already been described by several groups^{4,9,10} and we will only detail here the illumination procedure. The key point in doing near-field optics is to have enough light power concentrated on the object to study. Coherent light sources such as lasers are therefore well adapted to near-field optics thanks to the ease with which we can focus their power on a diffraction-limited micron-sized spot. When using an incoherent light source such as a lamp, the focusing procedure becomes more difficult because of the size of the source and the beam divergence. The illumination setup that we have built is depicted in Fig. 1. The light source is a 300 xenon-arc lamp (Cermax Model EX300-10F) with a built-in ellipsoidal reflector. The point light source is located at the first

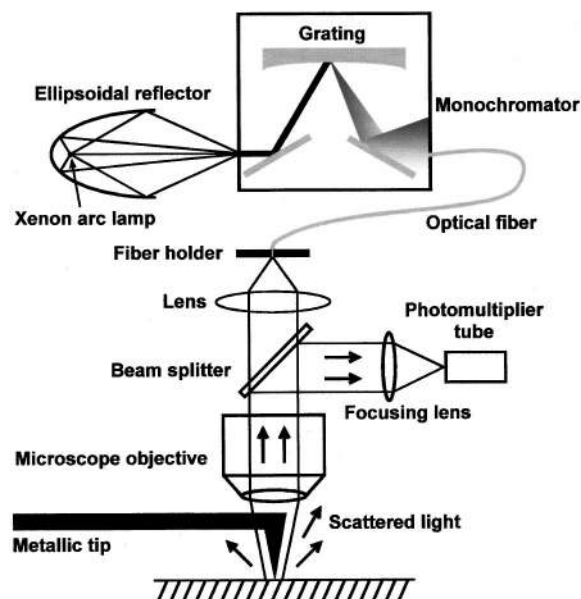


FIG. 1. Schematic diagram of the experimental setup.

^{a)}Author to whom correspondence should be addressed; electronic mail: aigouy@optique.espci.fr

^{b)}Also at Université Pierre et Marie Curie, 75231 Paris, France.

focus of the reflector. At the second focus, we have placed the entrance slits of a high numerical aperture monochromator (Instruments S.A., $F/n=2$, with concave holographic grating). A multi-mode optical fiber (Thorlabs Model FT-600-URT) was placed at the exit slits of the monochromator and connected to the focal zone of the tube lens of an optical microscope (Olympus BHM-363U). The outgoing light is focused onto the surface of the sample with a long working distance objective (Olympus MSPLAN50, numerical aperture (NA)=0.55). Within this configuration, we are able to concentrate an incoherent monochromatic light on a $10\text{-}\mu\text{m}$ -wide spot with a power density approximately equal to 1 W/cm^2 in a 1 nm spectral bandwidth. The tip is placed at the center of the spot and is made to vibrate in the tapping mode at a frequency close to 10 kHz with an amplitude of 50 nm . The light scattered by the tip and the specular reflection are collected in the far field by the objective used for illumination and a 50% beam splitter redirects the beam towards a photomultiplier tube (Hamamatsu R3878HA). A lock-in amplifier (EG&G Instruments Model DSP 7260) synchronized to the oscillation frequency of the tip allows us to extract the near-field optical signal. The far-field signal can also be measured simultaneously by a dc voltage amplifier.

The first question that is raised when performing near-field spectroscopy concerns the optical response of the probe itself. In our case, the tip is made of tungsten and its shape is conical. At first sight, this metal is particularly interesting to perform spectroscopy since its complex dielectric constant is relatively flat in the spectral range we use (from the UV to the near infrared).¹¹ However, even with a material having a flat spectral response, one can find that the coupling efficiency between the tip apex and the light depends on the wavelength. This spectral dependence can be explained by a quasiolestatic model. As shown in Ref. 12, the amplitude E_{det} of the field scattered by the tip at the detector position can be expressed as a function of the near field $E_{\text{exp}}(\mathbf{R}, z)$ illuminating the tip as follows:

$$\mathbf{E}_{\text{det}} \cdot \mathbf{j}_{\text{rec}} = \frac{-i\epsilon_0 c \lambda}{\pi} \int \left[\frac{\partial}{\partial z} \mathbf{E}_{\text{rec}}(\mathbf{R}, z) \right] \cdot \mathbf{E}_{\text{exp}}(\mathbf{R}, z) d\mathbf{R}, \quad (1)$$

where c is the speed of light in vacuum, ϵ_0 is the vacuum permittivity, and λ is the wavelength. $E_{\text{rec}}(\mathbf{R}, z)$ is the confined and enhanced electric field near the tip when illuminated by a hypothetical point source with unit current density \mathbf{j}_{rec} located at the detector position. In Eq. (1), the z axis is parallel to the tip axis and the integral is calculated in a plane at a constant z located below the tip. Recently, the field near a perfectly conducting conical tip has been introduced to model the local electric field in apertureless SNOM.¹³ In our case, both fields in Eq. (1), E_{rec} and E_{exp} can be modeled by the field in the vicinity of a perfectly conducting cone apex illuminated by a dipolar source.¹⁴ This model yields a wavelength dependence of these two fields like λ^{-v} where v is a constant smaller than unity which depends on the cone angle.¹⁴ Due to the interference between the field scattered by the tip E_{det} and the specular field, the signal at the detector is proportional to the amplitude of the scattered field E_{det} . Therefore, provided a perfectly conducting cone is a good model for a tungsten tip, the wavelength dependence of the signal predicted by Eq. (1) is λ^{1-2v} . The variations of the

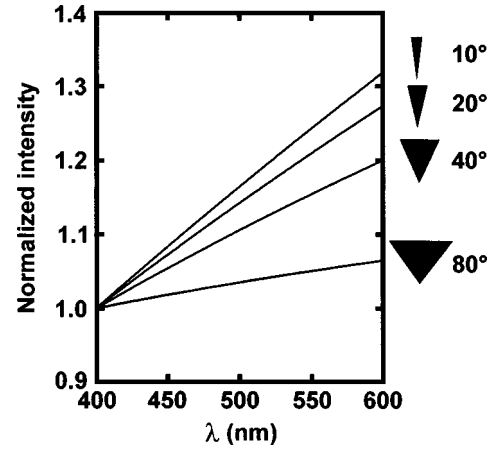


FIG. 2. Theoretical wavelength dependence of the signal for different values of the angle of the tip (10° , 20° , 40° , and 80°), modeled by a perfectly conducting cone.

predicted signal in the range $400\text{--}600\text{ nm}$ are plotted in Fig. 2 for different values of the total cone angle (10° , 20° , 40° , and 80°). For clarity, the curves have been normalized to the values of the signal at 400 nm . One can see that the tip geometry strongly influences the variations of the signal: the sharper the cone angle is, the stronger the variations are.

Next, we have tested experimentally the optical response of two tips as a function of the wavelength. Scanning electron micrographs of the tips are displayed in Fig. 3(a). Their total angles are approximately 26° (tip 1) and 43° (tip 2). We have measured the signal on a reference sample and normalized it by the specular far field. The reference sample is a UV-enhanced aluminum mirror with a reflection coefficient constant in this spectral range ($R=0.9$). The results are displayed in Fig. 3(b). For clarity, the spectra have been normalized to the experimental value at 400 nm . For both tips, the signal increases almost linearly with the wavelength, but with a different slope. This behavior is the same as that predicted theoretically and shown in Fig. 2. We have calculated

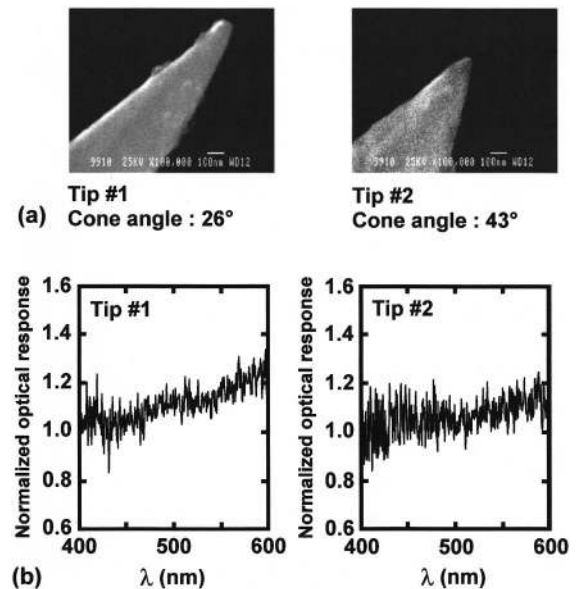


FIG. 3. (a) Scanning electron micrographs of two tips. Tips 1 and 2 have a 26° and 43° cone angle, respectively. (b) Experimental optical response of the two tips.

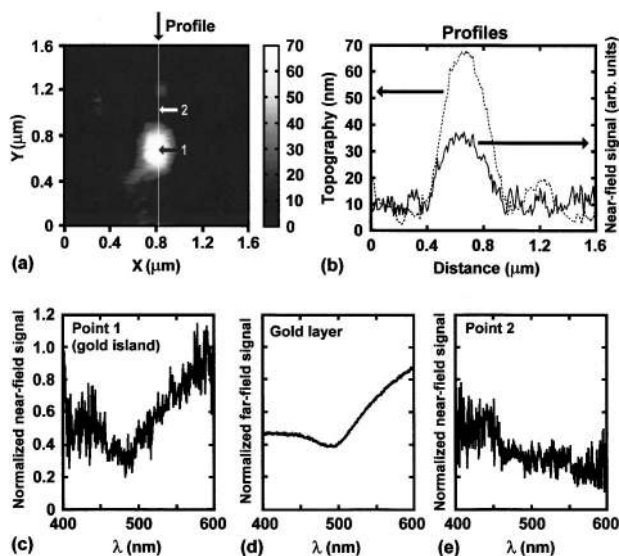


FIG. 4. (a) Topography of a gold island. (b) Topographic and near-field optical profiles of the gold island. The profiles are performed along the vertical white line indicated in Fig. 4(a). (c) Near-field optical spectrum measured on the gold island [arrow 1 in Fig. 4(a)]. (d) Far-field optical spectrum measured on a gold thin film. (e) Near-field optical spectrum measured at 100 nm away from the gold island [arrow 2 in Fig. 4(a)].

the mean slope in the spectral range 400–600 nm, after normalization of the signals by their value at $\lambda = 400$ nm. The experimental slopes are $(1.2 \pm 0.1) \times 10^{-3}$ for tip 1 and $(0.8 \pm 0.1) \times 10^{-3}$ for tip 2. The values of the slopes predicted theoretically by Eq. (1) (1.3×10^{-3} for tip 1 and 0.95×10^{-3} for tip 2) are in very good agreement with the experimental ones. Note that this increase of the scattered light intensity with the wavelength is specific to the conical shape. Modeling the tip apex by a small sphere (dipole) would yield a dependence of the signal like $1/\lambda^4$.¹⁵ Thus, the spectral behavior of the apertureless setup measured in this experiment is not described by a dipole model for the tip.

In order to find out if the method we have developed is reliable to achieve spectroscopic measurements, we have measured the optical response of a submicrometer-sized object: a gold island deposited on a SiO_2 substrate. An atomic force microscope image of the island is displayed in Fig. 4(a). Its dimensions are $\sim 400 \times 500$ nm with a height of ~ 65 nm. A vertical profile of the topography and its corresponding optical signal (measured at a constant wavelength: $\lambda = 535$ nm) are depicted in Fig. 4(b). A near-field optical spectrum has then been measured in the range 400–600 nm on the center of the island [indicated by arrow 1 in Fig. 4(a)]. The spectrum is displayed in Fig. 4(c). It has been normalized by a spectrum obtained on a reference sample (aluminum mirror: $R = 0.9$) with the same tip and in the same experimental conditions. This normalization is absolutely necessary because it allows: (i) to get rid of the light intensity variations emitted by the lamp when changing the wavelength, (ii) to take into account the absorption of the optical elements of the microscope, and (iii) to cancel the optical response of the tip. The spectrum obtained on the gold island [Fig. 4(c)] is similar to the one obtained in the far field on a continuous 30-nm-thick gold film [Fig. 4(d)]. The strong decrease of the signal in the range 600–500 nm is due to the absorption of light by electrons from the top of the d band to

the Fermi level.¹⁶ The similarity between the two spectra shows that, for this kind of island which has a relatively large size, there is neither a size-induced energy shift of the absorption edge nor a plasmon resonance peak. Such effects would appear on smaller islands like, for instance, the ones studied in Ref. 8. Finally, a spectrum obtained on the substrate, and more precisely at 100 nm from the island [indicated by arrow 2 in Fig. 4(a)], is presented in Fig. 4(e). At this special point, the spectrum does not exhibit any gold-related spectral feature, showing that the gold island, which is located only 100 nm away, did not influence the measurements. From this, we can deduce that the optical resolution is at least better than 100 nm.

In conclusion, we have developed a method to perform near-field optical spectroscopy which combines an apertureless SNOM, a xenon-arc lamp, and a monochromator. We have studied the optical response of the tip as a function of the wavelength. We have shown that the intensity of the light scattered by the tip increases with the wavelength and that these variations depend on the cone angle at the tip apex. A good agreement is obtained between the experimental spectra and theoretical predictions. A spectrum obtained on a gold island shows that the method is reliable to perform spectroscopy on submicrometer-sized objects, which would be very difficult to achieve by conventional far-field methods unless the islands were separated by several microns. This technique opens the way to perform local absorption spectroscopy and can find applications in various domains such as solid state physics, chemistry, and biology.

J.A.P., R.C., and J.J.G. acknowledge financial support from the TMR program Near-Field Optics for Nanotechnology from the European Union.

¹M. A. Paesler and P. J. Moyer, in *Near Field Optics: Theory, Instrumentation and Applications* (Wiley-Interscience, New York, 1996).

²E. A. Ash and G. Nichols, *Nature (London)* **237**, 510 (1972).

³U. Dürig, D. W. Pohl, and F. Rohner, *J. Appl. Phys.* **59**, 3318 (1986); E. Betzig, M. Isaacson, and A. Lewis, *Appl. Phys. Lett.* **51**, 2088 (1987); D. Courjon, K. Sarayeddine, and M. Spajer, *Opt. Commun.* **71**, 23 (1989); F. de Fornel, J. P. Goudonnet, L. Salomon, and E. Lesmiewska, *Proc. SPIE* **1139**, 77 (1989).

⁴A. Lahrech, R. Bachelot, P. Gleyzes, and A. C. Boccarda, *Appl. Phys. Lett.* **71**, 575 (1997).

⁵P. J. Moyer, C. L. Jahncke, M. A. Paesler, R. C. Reddick, and R. J. Warmack, *Phys. Lett. A* **145**, 343 (1990).

⁶C. L. Jahncke, M. A. Paesler, and H. D. Hallen, *Appl. Phys. Lett.* **67**, 2483 (1995).

⁷E. J. Sánchez, L. Novotny, and X. Sunney Xie, *Phys. Rev. Lett.* **82**, 4014 (1999).

⁸T. Klar, M. Perner, S. Grosse, G. von Plessen, W. Spirkel, and J. Feldmann, *Phys. Rev. Lett.* **80**, 4249 (1998).

⁹F. Zenhausern, M. P. O'Boyle, and K. H. Wickramasinghe, *Appl. Phys. Lett.* **65**, 1623 (1994).

¹⁰Y. Inouye and S. Kawata, *Opt. Commun.* **134**, 31 (1997).

¹¹*Handbook of Optics: Devices, Measurements and Properties*, 2nd ed. (McGraw-Hill, New York, 1995), Vol. II.

¹²J. A. Porto, R. Carminati, and J.-J. Greffet (unpublished).

¹³H. Cory, A. C. Boccarda, J. C. Rivoal, and A. Lahrech, *Microwave Opt. Technol. Lett.* **18**, 120 (1998).

¹⁴J. J. Bowman, T. B. A. Senior, and P. L. E. Uslenghi, in *Electromagnetic and Acoustic Scattering by Simple Shapes* (Hemisphere, New York, 1987), p. 662.

¹⁵M. Born and E. Wolf, in *Principles of Optics: Electromagnetic Theory of Propagation, Interference and Diffraction of Light*, 6th ed. (Cambridge University Press, Cambridge, England, 1980).

¹⁶M. L. Theye, *Phys. Rev. B* **2**, 3060 (1970).